Journal of Molecular Structure 1246 (2021) 131127

Contents lists available at ScienceDirect

Journal of Molecular Structure

journal homepage: www.elsevier.com/locate/molstr

Investigation of structural, electronical and *in vitro* cytotoxic activity properties of some heterocyclic compounds

Senem Akkoç[a,*], Burak Tüzün[b], Ayhan Özalp[c], Zülbiye Kökbudak[d]

[a] Suleyman Demirel University, Faculty of Pharmacy, Department of Basic Pharmaceutical Sciences, Isparta, 32260 , Turkey
[b] Cumhuriyet University, Faculty of Sciences, Department of Chemistry, Sivas, 58140, Turkey
[c] Erciyes University, Faculty of Medicine, Kayseri, 38039, Turkey
[d] Erciyes University, Faculty of Sciences, Department of Chemistry, Kayseri, 38039, Turkey

ARTICLE INFO

Article history:
Received 10 April 2021
Revised 26 June 2021
Accepted 15 July 2021
Available online 19 July 2021

Keywords:
ADME/T
DFT
Heterocyclic compound
Molecular docking

ABSTRACT

A series of heterocyclic compounds (**15**) were synthesized, characterized and tested towards two human cancer cell lines for learning their *in vitro* antiproliferative activities. Compound **3** demonstrated the most promising activity in breast cancer cell line with a half maximal inhibitory concentration (IC_{50}) value of 23.73 μM compared to other compounds (**1, 2, 4, 5**). Cytotoxic activity studies revealed that compounds **24** did not have antiproliferative activity towards liver cancer cell line. Computational methods were used to determine various quantum chemical parameters in order to identify correlations with the measured biological activity, which can assist in the molecular modeling of new heterocyclic systems. The biological activities of heterocyclic molecules against cancer cell proteins that are the crystal structure of the BRCT repeat region from the breast cancer-associated protein, ID: 1JNX, crystal structure of VEGFR kinase (liver cancer) protein, ID: 3WZE, and crystal structure of an allosteric Eya2 phosphatase inhibitor (lung cancer) protein, ID: 5ZMA, were compared. Finally, ADME/T analysis was performed for heterocyclic molecules and their future possibilities as a drug were investigated.

1. Introduction

It is thought that deaths from cancer will soon surpass deaths from cardiovascular diseases [1,2]. There are many types of cancer at present. Of these, breast cancer is one of the most common cancer types worldwide and is seen as the fifth most common cause of cancer-related deaths. However, there are different treatment methods such as surgery, chemotherapy, radiotherapy, immunotherapy and hormone therapy, which are chosen based on the stage, size, aggressiveness, grade, metastatic behavior, and overall health, age, menopausal status, and intrinsic molecular subtyping of tumor [1,3]. Due to the increasing incidence of breast cancer, which ranks first among cancer-related deaths in women, the search for effective drug candidate molecules for this type of cancer should continue rapidly.

Liver cancer is a type of cancer that causes an increase in the number of cancer-related deaths worldwide. It is estimated to be the sixth most common cancer globally and the fourth leading cause of cancer deaths, with an estimated 841,000 new cases and 782,000 deaths annually [4,5]. This type of cancer, which affects both women and men, is more common in men. Moreover, liver cancer ranks second in deaths for males. There are different types of primary liver cancer. Hepatocellular carcinoma (HCC) is the most common type, which occurs most often in people with risk factors, such as cirrhosis caused by hepatitis B or hepatitis C infection, obesity, smoking, heavy alcohol intake, and Type 2 diabetes [6]. The second one is intrahepatic cholangiocarcinoma. The open structures of some drugs used in the treatment of breast and liver cancers are given below in Fig. 1.

In this work, for the reasons mentioned above, a series of heterocyclic compounds (**1–5**) were synthesized in order to find effective drug candidate molecules against cancer, a considerable disease today. These compounds (**1–5**) were screened towards the human breast cancer cell line and human liver cancer cell line for 48 h. The biological activity, measured from the IC_{50} parameter, was determined *in vitro* and the results compared with several quantum chemical parameters, such as E_{HOMO}, E_{LUMO}, electronegativity (χ), chemical hardness (η), electrophilicity (ω), global softness (σ), and nucleophilicity (ε), obtained from various computational methods in order to identify correlations that assist in the modeling of new systems.

* Corresponding author.
E-mail address: senemakkoc@sdu.edu.tr (S. Akkoç).

https://doi.org/10.1016/j.molstruc.2021.131127
0022-2860/

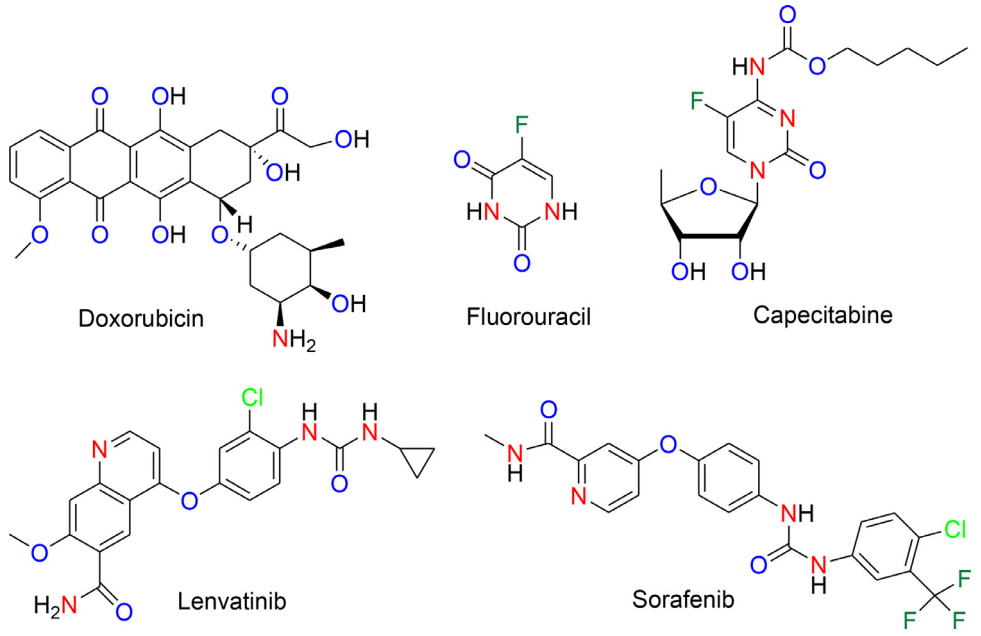

Fig. 1. The open structures of a few commercial drugs used in the treatment of some types of cancer.

2. Methods

2.1. Reagent and materials

The tools and devices used during the experiments are as follows: Gemini-Varian 200 MHz NMR spectrophotometer, Shimadzu 435 V-04 model IR spectrometer, EA1108 CHNS-brand elemental analysis device, Buchi 510 brand melting point device, Camag brand thin layer chromatogram device (254/366 nm), and DC Alufolien Kieselgel 60/254 Merck TLC boards.

2-Acetylnaphthalene, 4–hydroxy-4-(naphthalen-2-yl)but–3-en-2-one, *p*-toluidine, 2-nitroaniline, α-naphthylamine, 4-nitrophenylhydrazine, 2,4-dinitrophenylhydrazine, sodium amide, acetic acid, ethyl acetate, diethyl ether, benzene, toluene were purchased from Sigma-Aldrich or Merch chemical firms.

Human breast adenocarcinoma cell line (MDA-MB-231) (ATCC® HTB-26^{TM}) and human liver hepatocellular carcinoma cell line (HepG2) (ATCC® HB-8065^{TM}) were purchased from American Type Culture Collection (ATCC, USA). Dulbecco's modified eagle's medium high glucose (DMEM), fetal bovine serum (FBS), 3-(4,5-dimethylthiazol-2-yl)−2,5-diphenyl tetrazolium bromide (MTT), phosphate buffered saline (PBS) and pentahydrate (bis-benzimide) for the cell culture studies were purchased from Sigma (Sigma-Aldrich, USA), Gibco (Life Technologies, USA), ThermoFisher Scientific, Isolab Laborgerate GmbH (Germany), or Jet Biofil (Pathtech, China).

2.2. Synthesis of compounds

2.2.1. Synthesis of 1-(naphthalen-2-yl)butane-1,3-dione

2-Acetylnaphthalene (8.51 g) was dissolved in 20 mL of ethyl acetate and mixed. 40 ml of diethyl ether as solvent was added to the reaction medium. Sodium amide ($NaNH_2$) (1.95 g) was slowly put into the reaction medium. The reaction was conducted at 0 °C for 1 h and then carried out at room temperature for 24 h. The precipitated white crystals were filtered and washed with diethyl ether. The product was dried. It was dissolved in 150 ml of pure distilled water and filtered from filter paper, and 50% acetic acid (HAc) solution was added to the filtrate until the medium was acidic. Crystals growing in the solution were filtered. It was washed with water and dried. The product was recrystallized in petroleum ether [7,8]. Yield: 28%, m.p.: 77–78 °C. The synthesis reaction of 1-(naphthalen-2-yl)butane-1,3–dione are given in Scheme 1.

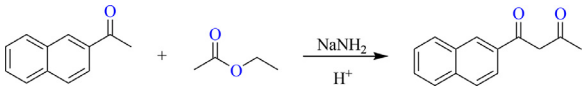

Scheme 1. Synthesis of starting matter.

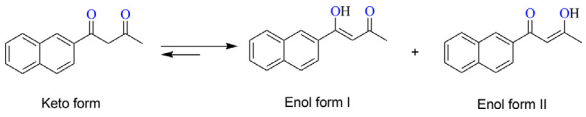

Scheme 2. Keto and enol forms of starting matter.

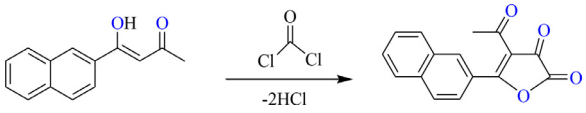

Scheme 3. Synthesis of 4-acetyl-5-(naphthalen-2-yl)furan-2,3–dione.

2.2.2. Synthesis of 4-acetyl-5-(naphthalen-2-yl)furan-2,3-dione

4-Hydroxy-4-(naphthalen-2-yl)but–3-en-2-one (1.5 g, 1 mmol) was added to a dry reaction balloon, and 22 ml of diethyl ether was put to over. When the homogeneous solution was prepared by shaking slowly for a few minutes, freshly distilled phosgene ($COCl_2$) (0.606 ml, 1 mmol) was added. After the reaction was completed, red color crystals formed in the solution which was kept at room temperature for 48 h in a dark place. The crystals were filtered and washed with diethyl ether. It was dried in a vacuum desiccator on phosphorus pentoxide (P_2O_5) [8]. Yield: 39%, m.p.: 110–111 °C. The keto and enol forms of the starting matter used are given in the Scheme 2. The synthesis reaction of 4-acetyl-5-(naphthalen-2-yl)furan-2,3–dione are given in Scheme 3.

Five heterocyclic compounds namely 3-acetyl-4-(2-naphthyl)−4-(*p*-toludino)−2-oxo-3-butenoic acid **(1)**, 3-acetyl-

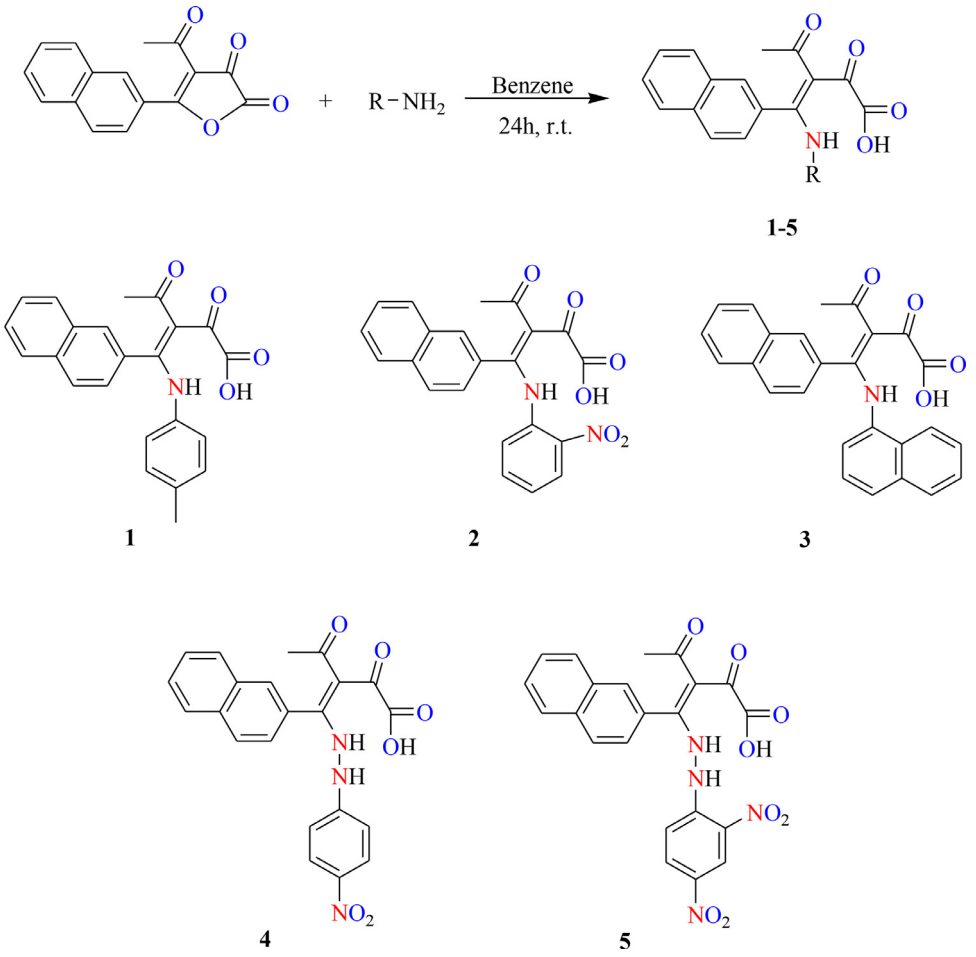

Scheme 4. The open structure of heterocyclic compounds **1–5**.

4-(2-naphthyl)–4-(2-nitroanilino)–2-oxo-3-butenoic acid **(2)**, 3-acetyl-4-(2-naphthyl)–4-(1-naphthylamino)–2-oxo-3-butenoic acid **(3)**, 3-acetyl-4-(2-naphthyl)–4-(4-nitrophenylhydrazino)–2-oxo-3-butenoic acid **(4)**, 3-acetyl-4-(2-naphthyl)–4-(2,4-dinitrophenylhydrazino)–2-oxo-3-butenoic acid **(5)** were synthesized using 4-acetyl-5-(naphthalen-2-yl)furan-2,3-dione. The open structures of compounds are given in Scheme 4.

*3-Acetyl-4-(2-naphthyl)–4-(*p*-toludino)–2-oxo-3-butenoic acid, 1*

4-Acetyl-5-(naphthalen-2-yl)furan-2,3–dione (0.3 g, 1 mmol) was dissolved in 50 ml of benzene, and *p*-toluidine (0.12 g, 1 mmol) was added to over. The reaction was conducted at room temperature for 24 h. The light yellow precipitate formed was filtered off and crystallized in toluene. Yield: 68%, m.p.: 119–120 °C. FT-IR ν (cm^{-1}): 3600–3100 (O-H, N-H), 1680–1560 ($C=O$), 1480 (N-H). ^{1}H NMR (200 MHz, DMSO–d_6, 293 K, ppm), δ: 10.60 (s, 1H, OH), 8.41 (1H, NH), 6.95–7.97 (m, 11H, Ar-H), 2.49 (s, 3H, Ar-CH_3), 2.12 (s, 3H, CH_3CO). Elemental analysis for $C_{23}H_{19}NO_4$ (373.4 g/mol)%: Found C: 73.54, H: 5.03, N: 3.75. Anal. Calc. C: 73.98, H: 5.13, N: 3.75.

3-Acetyl-4-(2-naphthyl)–4-(2-nitroanilino)–2-oxo-3-butenoic acid, 2

4-Acetyl-5-(naphthalen-2-yl)furan-2,3–dione (0.3 g, 1 mmol) was dissolved in 50 ml of benzene, and 2-nitroaniline (0.156 g, 1 mmol) was added to over. The reaction was conducted for 24 h at room temperature. The precipitate formed was filtered off and crystallized in toluene. Yield: 65%, m.p.: 170–171 °C. FT-IR ν (cm^{-1}): 3700–3400 (O–H), 3400 (N–H), 1700–1650 ($C=O$), 1510 (N–H). ^{1}H NMR (200 MHz, DMSO–d_6, 293 K, ppm), δ: 10.21 (s, 1H, OH), 8.50 (1H, NH), 6.57–8.01 (m, 11H, Ar-H), 2.52 (s, 3H, CH_3CO). Elemental analysis for $C_{22}H_{16}N_2O_6$ (404.37 g/mol)%: Found C: 64.55, H: 4.04, N: 6.69. Anal. Calc. C: 65.34, H: 3.99, N: 6.93.

3-Acetyl-4-(2-naphthyl)–4-(1-naphthylamino)–2-oxo-3-butenoic acid, 3

4-Acetyl-5-(naphthalen-2-yl)furan-2,3–dione (0.3 g, 1 mmol) was dissolved in 50 ml of benzene, and α-naphthylamine (0.16 g, 1 mmol) was added to over. The reaction was conducted for 24 h at room temperature. The orange precipitate formed was filtered off and crystallized in toluene. Yield: 64%, m.p.: 130–131 °C. FT-IR ν (cm^{-1}): 3500–3200 (O–H), 1680–1580 ($C=O$), 1480 (N–H). ^{1}H NMR (200 MHz, DMSO–d_6, 293 K, ppm), δ: 10.43 (s, 1H, OH), 8.23 (1H, NH), 7.20–8.00 (m, 14H, Ar-H), 2.55 (s, 3H, CH_3CO). Elemental analysis for $C_{26}H_{19}NO_4$ (409.43 g/mol)%: Found C: 76.01, H: 4.99, N: 3.33. Anal. Calc. C: 76.27, H: 4.68, N: 3.42.

3-Acetyl-4-(2-naphthyl)–4-(4-nitrophenylhydrazino)–2-oxo-3-butenoic acid, 4

4-Acetyl-5-(naphthalen-2-yl)furan-2,3–dione (0.3 g, 1 mmol) was dissolved in 50 ml of benzene, and 4-nitrophenylhydrazine (0.173 g, 1 mmol) was added to over. The reaction was conducted for 24 h at room temperature. The orange precipitate formed was filtered off and crystallized in toluene. Yield: 36%, m.p.: 195–196 °C. FT-IR ν (cm^{-1}): 3600–3100 (O–H, N–H), 1720–1650 ($C=O$), 1490 (N–H). ^{1}H NMR (200 MHz, DMSO–d_6, 293 K, ppm), δ: 10.58 (s, 1H, OH), 8.46–8.43 (dd, 2H, NH), 7.57–8.00 (m, 11H, Ar-H), 2.65

(s, 3H, CH_3CO). Elemental analysis for $C_{22}H_{17}N_3O_6$ (419.39 g/mol)%: Found C: 63.46, H: 3.95, N: 10.39. Anal. Calc. C: 63.01, H: 4.09, N: 10.02.

3-Acetyl-4-(2-naphthyl)–4-(2,4-dinitrophenylhydrazino)–2-oxo-3-butenoic acid, 5

4-Acetyl-5-(naphthalen-2-yl)furan-2,3–dione (0.3 g, 1 mmol) was dissolved in 50 ml of benzene, and 2,4-dinitrophenylhydrazine (0.22 g, 1 mmol) was added to over. The reaction was conducted at room temperature for 24 h. The orange precipitate formed was filtered off and crystallized in toluene. Yield: 58%, m.p.: 179–180 °C. FT-IR ν (cm^{-1}): 3600–3100 (O–H, N–H), 1660–1580 ($C=O$), 1500–1480 (N–H). ^1H NMR (200 MHz, DMSO–d_6, 293 K, ppm), δ: 10.85 (s, 1H, OH), 8.96–8.78 (dd, 2H, NH), 7.57–7.99 (m, 10H, Ar-H), 2.63 (s, 3H, CH_3CO). Elemental analysis for $C_{22}H_{16}N_4O_8$ (464.38 g/mol)%: Found C: 57.41, H: 3.57, N: 11.67. Anal. Calc. C: 56.90, H: 3.47, N: 12.06.

2.3. In vitro *cytotoxic activity studies*

The cytotoxic activity studies were done according to the literature procedures [9,10]. The MDA-MB-231 and HepG2 cells were seeded into sterile 96-well plates at a density of 5×10^3 cells/well. After 24 h, cells were exposed to developed compounds at six different concentrations for 48 h. After this period was completed, 5 mg/mL of MTT stock solution was added to each well, and plates were incubated for 3 h. The measure of absorbance values was done using the Promega plate reader device at 560 nm. IC_{50} values were calculated using GraphPad Prism software 5.

2.4. Theoretical methods

2.4.1. Quantum chemical descriptors study

In this study, Hartree-Fock (HF) [11,12] and DFT calculations with B3LYP [13,14] and M06–2X [15] functionals, and 3–21 G, 6–31 G, and SDD basis set, were performed with Gaussian09 RevD.01 [16] and the results obtained with GaussView 5.0.8, ChemDraw 15.1 and Chemcraft V1.8 programs [17-19]. Many quantum chemical parameters of molecules can be calculated on these basis sets. Within this parameter, two parameters stand out more than other parameters. The most important of these parameters are the HOMO (Highest Occupied Molecular Orbital) and LUMO (Lowest Unoccupied Molecular Orbital) parameters, which can be used to describe the activity of the molecules. The HOMO-LUMO energy gap, chemical potential (μ), electrophilicity (ω), chemical hardness (η), global softness (σ), nucleophilicity (ε) parameters can be obtained from quantum chemical calculations, obtained with the following equations (1–7) [20,21]: ionization energy (I) and electron affinity (A) of molecules are calculated with HOMO and LUMO energy.

$$\chi = -\left(\frac{\partial E}{\partial N}\right)_{\upsilon(r)} = \frac{1}{2}(I+A) \cong -\frac{1}{2}(E_{HOMO} + E_{LUMO})$$

$$\eta = -\left(\frac{\partial^2 E}{\partial N^2}\right)_{\upsilon(r)} = \frac{1}{2}(I-A) \cong -\frac{1}{2}(E_{LUMO} - E_{HOMO})$$

$$\sigma = 1/\eta,\ \omega = \chi^2/2\eta,\ \varepsilon = 1/\omega$$

2.4.2. Molecular docking calculations

It is an important method used to compare molecules' biological activities against proteins with molecular docking calculations. With this method, a comparison can be made with the protein interaction parameters' numerical value with any molecule studied. These parameters are important to explain the biological activities of molecules theoretically.

Table 1
IC_{50} results of heterocyclic compounds against cell lines.

Compounds	IC_{50} (μM)	
	MDA-MB-231	HepG2
1	192.20	168.80
2	93.32	297.60
3	**23.73**	231.40
4	143.40	275.90
5	199.30	201.50
Cisplatin	7.11	40.45

Molecular docking to calculate heterocyclic compounds' biological activity was performed using the Maestro Molecular Modeling Platform (MMMP) (version 12.2) by Schrödinger. Proteins and heterocyclic compounds are prepared for calculations using the MMMP program mentioned above. The Gaussian software program [16] was used to obtain molecules' optimized structures and all calculations were done with the MMMP, LLC [22]. The MMMP by Schrödinger comes together from many modules. The protein preparation module [23,24] was used in the first module. In the subsequent module, the LigPrep module [25,26] was used to prepare the heterocyclic compounds for calculations.

The Glide ligand docking module [27] was used to interact with the molecule and proteins. The OPLS3e method was used in docking calculations of molecules and proteins in all modules used. The Qik–prop module [28] of the Schrödinger software was used for ADME/T analysis.

3. Result and discussion

3.1. Synthesis

Five different compounds (**1–5**) were synthesized by conducting experiments with Claisen-Schmidt, aldol, cycloadition and nucleophilic addition reactions. All compounds were characterized by IR, NMR and elemental analysis. Peaks belonging to functional groups in the molecule were seen in the IR spectra. The accuracy of the structures has also been proven with the NMR spectrum. Finally, the structure and purity of the compounds were confirmed by elemental analysis.

3.2. In vitro *cytotoxic activity studies*

The cytotoxic activities of molecules were evaluated at 5, 10, 20, 50, 100, and 200 μM concentrations towards two human cell lines, including MDA-MB-231 and HepG2 for 48 h. The results are given in Table 1.

Cisplatin is currently used clinically to treat breast cancers, and this positive control drug used in this study showed high cytotoxicity in the MDA-MB-231 cell line as expected. The most effective compound among **1–5** after the positive control was found to be molecule **3** with an IC_{50} value of 23.73 μM in MDA-MB-231. This result demonstrated that the substituents on the molecule play a significant role in activity. Other compounds (**1, 2, 4, 5**) showed *in vitro* cytotoxic activity in breast cancer with IC_{50} values of 192.20, 93.32, 143.40 and 199.30 μM, respectively, albeit very less than molecule **3**.

The antiproliferative activities of **1–5** were examined as *in vitro* towards the HepG2 cell line (Table 1). The results in Table 1 revealed that compounds **2–5** were inactive against HepG2 at the concentrations tested (5–200 μM) and their IC_{50} values were higher than 200 μM. Compound **1** indicated higher cytotoxic activity in the liver cell line than others, but the related molecule was found to have an IC_{50} value higher than 100 μM. Thus, all the com-

Table 2

	E_{HOMO} (eV)	E_{LUMO} (eV)	ΔE (eV)	η (eV)	σ (eV^{-1})	χ (eV)	ω (eV)	ε (eV^{-1})	Dipole (D)
B3LYP/3–21 g LEVEL									
1	−5.8731	−2.4303	3.4428	1.7214	0.5809	4.1517	5.0065	0.1997	5.7979
2	−6.2930	−3.0529	3.2401	1.6200	0.6173	4.6729	6.7394	0.1484	6.5164
3	−5.8576	−2.4988	3.3587	1.6794	0.5955	4.1782	5.1976	0.1924	4.8734
4	−6.5155	−2.9897	3.5258	1.7629	0.5672	4.7526	6.4064	0.1561	7.4366
5	−6.8432	−3.2869	3.5563	1.7781	0.5624	5.0650	7.2139	0.1386	7.9138
B3LYP/6–31 g LEVEL									
1	−5.8723	−2.6978	3.1745	1.5873	0.6300	4.2850	5.7840	0.1729	7.0797
2	−6.4230	−3.2722	3.1508	1.5754	0.6348	4.8476	7.4581	0.1341	9.3830
3	−5.9950	−2.6817	3.3133	1.6566	0.6036	4.3383	5.6805	0.1760	5.5736
4	−6.4810	−3.1633	3.3176	1.6588	0.6028	4.8222	7.0090	0.1427	6.4243
5	−6.5580	−3.5968	2.9612	1.4806	0.6754	5.0774	8.7061	0.1149	6.0719
B3LYP/SDD LEVEL									
1	−6.1664	−2.9350	3.2314	1.6157	0.6189	4.5507	6.4088	0.1560	7.3678
2	−6.6007	−3.5337	3.0670	1.5335	0.6521	5.0672	8.3718	0.1194	9.9689
3	−6.1621	−2.9035	3.2586	1.6293	0.6138	4.5328	6.3052	0.1586	5.9374
4	−6.6440	−3.4110	3.2330	1.6165	0.6186	5.0275	7.8180	0.1279	6.7682
5	−6.7735	−3.9234	2.8501	1.4251	0.7017	5.3484	10.0366	0.0996	6.6065
HF/3–21 g LEVEL									
1	−8.3550	1.5176	9.8726	4.9363	0.2026	3.4187	1.1838	0.8447	6.2777
2	−8.3632	0.5714	8.9347	4.4673	0.2238	3.8959	1.6988	0.5887	8.6598
3	−8.2065	1.0640	9.2704	4.6352	0.2157	3.5713	1.3758	0.7269	5.5416
4	−8.6201	1.1037	9.7238	4.8619	0.2057	3.7582	1.4525	0.6885	7.2775
5	−8.7085	0.2087	8.9172	4.4586	0.2243	4.2499	2.0255	0.4937	5.9699
HF/6–31 g LEVEL									
1	−8.5891	1.5176	10.1067	5.0533	0.1979	3.5357	1.2370	0.8084	12.6711
2	−8.4753	0.5714	9.0468	4.5234	0.2211	3.9519	1.7263	0.5793	10.2220
3	−8.1436	1.0640	9.2076	4.6038	0.2172	3.5398	1.3609	0.7348	6.1338
4	−8.4027	1.1037	9.5064	4.7532	0.2104	3.6495	1.4010	0.7138	9.4100
5	−8.6054	0.2087	8.8141	4.4071	0.2269	4.1983	1.9998	0.5001	6.1730
HF/SDD LEVEL									
1	−8.7303	1.1932	9.9235	4.9618	0.2015	3.7685	1.4311	0.6987	12.8224
2	−8.6155	0.3815	8.9970	4.4985	0.2223	4.1170	1.8839	0.5308	10.4115
3	−8.3050	0.8759	9.1809	4.5905	0.2178	3.7145	1.5029	0.6654	6.2746
4	−8.6721	0.4142	9.0862	4.5431	0.2201	4.1290	1.8763	0.5330	9.4418
5	−8.7406	−0.0871	8.6536	4.3268	0.2311	4.4139	2.2513	0.4442	6.2747
M062X/3–21 g LEVEL									
1	−7.1599	−1.5595	5.6004	2.8002	0.3571	4.3597	3.3939	0.2946	5.9579
2	−7.6190	−2.0215	5.5974	2.7987	0.3573	4.8203	4.1510	0.2409	8.4301
3	−7.5591	−1.6172	5.9419	2.9710	0.3366	4.5881	3.5428	0.2823	10.0367
4	−7.9071	−2.1546	5.7525	2.8763	0.3477	5.0309	4.3998	0.2273	7.3849
5	−8.1322	−2.3895	5.7427	2.8714	0.3483	5.2608	4.8193	0.2075	5.2139
M062X/6–31 g LEVEL									
1	−7.2791	−1.7584	5.5207	2.7603	0.3623	4.5188	3.6987	0.2704	−7.2791
2	−7.5134	−2.1938	5.3196	2.6598	0.3760	4.8536	4.4284	0.2258	−7.5134
3	−7.3001	−1.7334	5.5667	2.7833	0.3593	4.5167	3.6648	0.2729	−7.3001
4	−8.0233	−2.2161	5.8072	2.9036	0.3444	5.1197	4.5136	0.2216	−8.0233
5	−7.7923	−2.5084	5.2839	2.6420	0.3785	5.1503	5.0201	0.1992	−7.7923
M062X/SDD LEVEL									
1	−7.4971	−2.0058	5.4913	2.7457	0.3642	4.7514	4.1112	0.2432	7.3206
2	−7.6799	−2.5192	5.1607	2.5803	0.3875	5.0996	5.0392	0.1984	9.0942
3	−7.5033	−1.9688	5.5346	2.7673	0.3614	4.7360	4.0527	0.2467	5.8879
4	−7.9055	−2.4346	5.4709	2.7354	0.3656	5.1701	4.8858	0.2047	8.8513
5	−7.9749	−2.8798	5.0951	2.5475	0.3925	5.4274	5.7813	0.1730	4.0234

*Abbreviations given in the table: chemical potential (μ), electronegativity (χ), electrophilicity (ω), chemical hardness (η), global softness (σ), and nucleophilicity (ε).

pounds demonstrated less efficacy than the standard drug cisplatin used against both cell lines. Dose-dependent antiproliferative effect changes of the molecules (**1 5**) are given in Figs. 2 and 3 below.

Figs. 2 and 3 show that the effects of compounds **1–5** against proliferation vary partly depending on concentration. At 5 µM concentration of the compounds **1–5** and cisplatin, viability ratio was obtained as 96.15%, 90.08%, 63.80%, 94.14%, 99.85% and 50.85% in MDA-MB-231 cells, respectively. On the other hand, the viability rate of MDA-MB-231 cells was obtained as 45.15%, 47.52%, 31.60%, 45.71%, 27.64% and 14.14% at a 200 µM concentration of **1–5** and cisplatin, respectively. These results show that breast cancer cell proliferation is affected by the prepared drugs' concentration (Fig. 2). It is clear that even if there is no sharp decrease in the

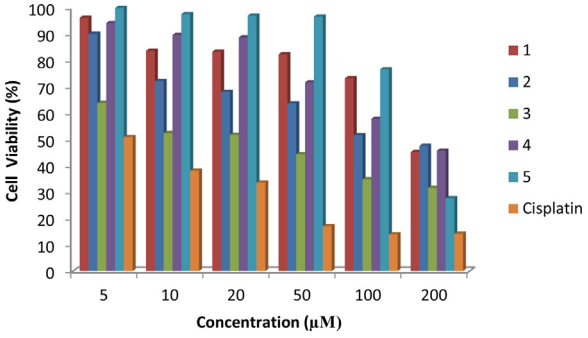

Fig. 2. Dose-dependent antiproliferative effect of compounds **1–5** on MDA-MB-231 cells for 48 h.

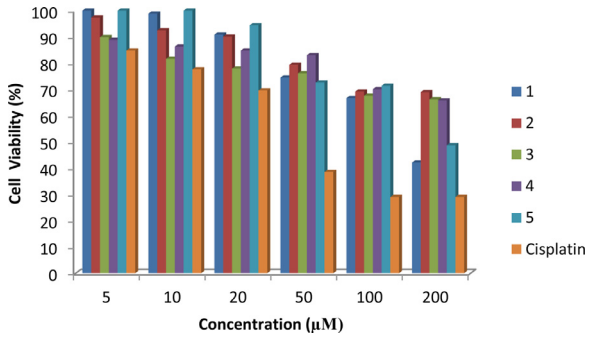

Fig. 3. Dose-dependent antiproliferative effect of compounds **1–5** on HepG2 cells for 48 h.

proliferation of cells when the drug concentration is changed from 5 µM to 10 µM in Fig. 3, the cells are affected by this concentration change. When 200 µM concentration was reached, it was seen that cell viability was severely affected by concentration change and viability ratios were obtained as 42.13%, 68.95%, 66.21%, 65.77%, 48.73% and 29.01% for **1–5** and cisplatin, respectively, (Fig. 3).

3.3. Theoretical results

A lot of parameters are found from the calculations made to compare the chemical activities of molecules. The most critical parameters among the obtained are HOMO and LUMO parameters. According to the Koopmans' (HF) and Janak (DFT) theorems, which make it possible to estimate the ionization energies (I) and electronic affinity (A), a positive energy for HOMO indicates an unbound electron. This result (and according to the data in Table 2, which reinforces this statement) suggests that there may have been an exchange between HOMO and LUMO energy values. In this case, the text refers to a positive energy for LUMO, which indicates that the molecular system has low electron affinity. The molecule with the lowest numerical value of the LUMO parameter has the highest chemical activity because the molecule will give more electrons. However, the other parameters' numerical values are calculated from the HOMO and LUMO parameters' numerical values. The numerical values of all parameters obtained for molecules are given in Table 2.

The figural representation of some parameters is given in Fig. 4. In the first picture, optimized structures of molecules are given for each molecule. In the second picture, the HOMO energy orbitals of the molecules are shown. In the following picture, LUMO orbitals of the molecules are given. The Electrostatic Potentials (ESP) of the molecules are demonstrated in the last picture.

The parameters obtained with calculations provide significant information about the chemical properties of molecules. There are two important points that determine chemical activity. One of them is the ability to donate electrons, and the other is the ability to receive electrons. The HOMO and ESP shapes of the molecules provide information about their electron densities. The places where HOMO orbitals are dense and the red regions showing the ESP of the molecule are suitable regions for electrophile attack.

The electronegativity numerical value of the molecules shows the strength of the atoms in the molecule to attract the bond electrons. The bond electrons of the molecules with higher electronegativity numerical value will be more attracted by the atoms in the molecule. Hence, the activity of the molecule decreases. However, chemical hardness can be conceptualized as the barrier to the disruption of the electron cloud of any chemical species, namely atoms, ions, or molecules. Chemical hardness is an important parameter that helps to explain many chemical properties such as solubility of molecules, chemical reactivity and complex stability. The opposite of chemical hardness is global softness.

Table 3
Numerical values of the docking parameters of molecules against cancer proteins.

Breast cancer	**1**	**2**	**3**	**4**	**5**
Docking Score	−3.27	−3.69	−3.20	−3.82	−3.19
Glide ligand efficiency	−0.12	−0.12	−0.10	−0.12	−0.09
Glide hbond	−0.06	−0.38	−0.36	−0.36	−0.42
Glide evdw	−23.73	−24.12	−24.08	−30.48	−25.76
Glide ecoul	−3.25	−8.09	−6.53	−2.90	−8.02
Glide emodel	−34.49	−39.53	−37.48	−42.75	−39.44
Glide energy	−26.98	−32.21	−30.60	−33.39	−33.78
Glide Einternal	1.51	2.42	3.87	7.81	2.31
Liver cancer	**1**	**2**	**3**	**4**	**5**
Docking Score	−5.97	−5.84	−5.70	−4.55	–
Glide ligand efficiency	−0.19	−0.19	−0.18	−0.16	–
Glide hbond	−0.51	−0.33	−0.38	−0.23	–
Glide evdw	−35.07	−40.29	−42.81	−29.99	–
Glide ecoul	−3.88	−3.95	−5.56	−0.68	–
Glide emodel	−50.19	−60.51	−65.43	−40.31	–
Glide energy	−38.96	−44.24	−48.37	−30.67	–
Glide einternal	6.79	7.63	5.15	2.68	–
Lung cancer	**1**	**2**	**3**	**4**	**5**
Docking Score	−3.96	–	–	−3.55	–
Glide ligand efficiency	−0.13	–	–	−0.13	–
Glide hbond	0.00	–	–	−0.16	–
Glide evdw	−39.64	–	–	−31.13	–
Glide ecoul	3.59	–	–	−0.24	–
Glide emodel	−39.02	–	–	−34.05	–
Glide energy	−36.05	–	–	−31.37	–
Glide einternal	7.71	–	–	3.98	–

3.4. Docking studies

Molecular docking calculations are done using optimized structures of molecules obtained from quantum chemical calculations [29,30]. Many parameters are obtained from the interactions of molecules against proteins. The most important factor increasing the biological activity of molecules against proteins is interaction such as hydrogen bonds, polar, hydrophobic interactions, π-π and halogen [31–33]. As a result of the calculations made, these interactions between the molecule with the highest biological activity value and proteins are shown in Figs. 5 7. Other images are given in supplementary data in Figures S1-S8.

The numerical values of the parameters obtained from of molecules' interactions against cancer proteins are given in Table 3. Some parameters related to the biological activities of the molecules were calculated and shown in this table. The most important of these parameters is the docking score. The molecule with the most negative numerical value of this parameter has the highest biological activity value. It is well known that the most crucial factor affecting the biological activities of these molecules is interaction [34]. As the interaction of molecules with proteins increases, the biological activity value of the molecule increases. All other parameters provide other numerical data about this interaction. Parameters such as Glide hbond, Glide evdw, and Glide ecoul give numerical values of important chemical bonds and interactions between molecules and protein [35]. On the other hand, parameters such as Glide emodel, Glide energy, and Glide einternal give quantitative data about the exposure that occurs due to the interaction between molecules and proteins.

After the studied molecules interacted with cancer proteins, ADME/T analysis was performed to use the molecules as advanced drugs. With this analysis, the behavior of molecules in human

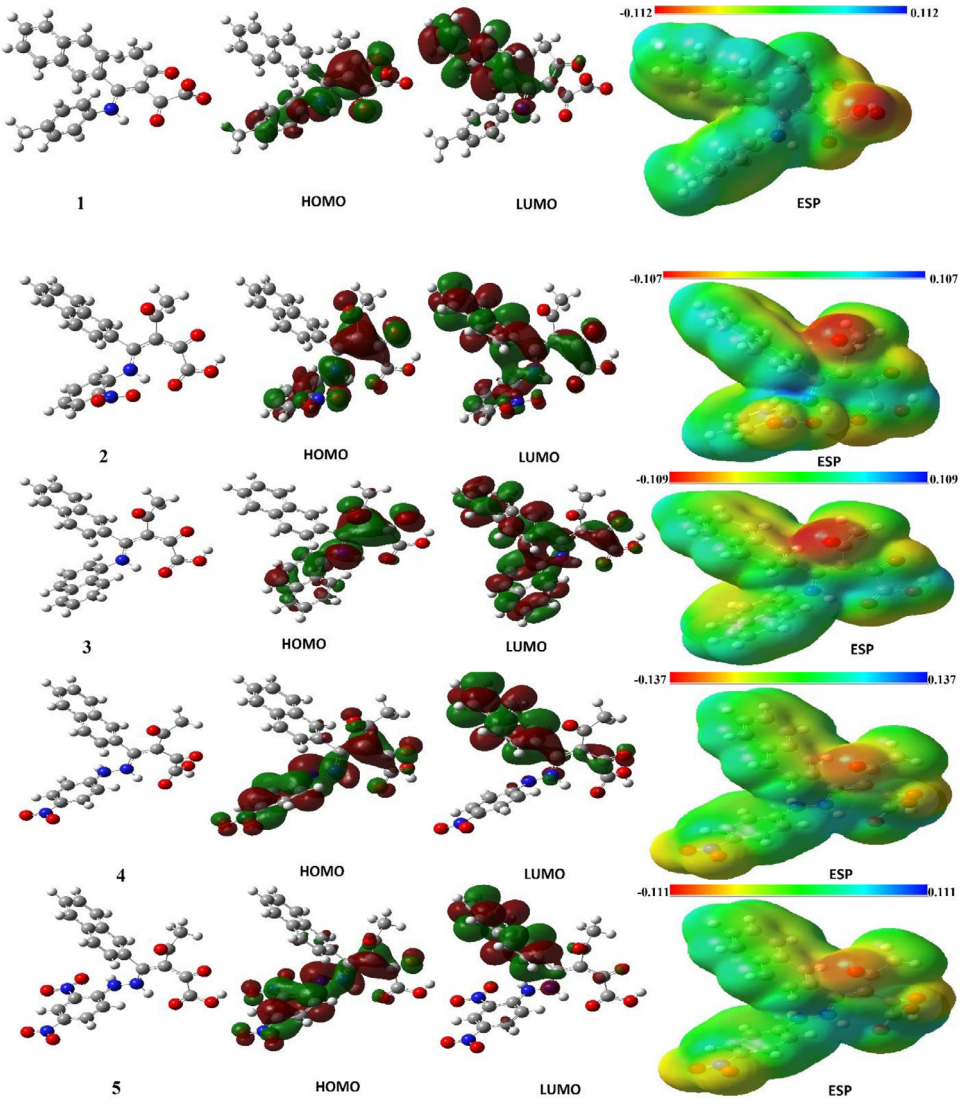

Fig. 4. Representations of optimized structures, HOMO, LUMO, and ESP of molecules.

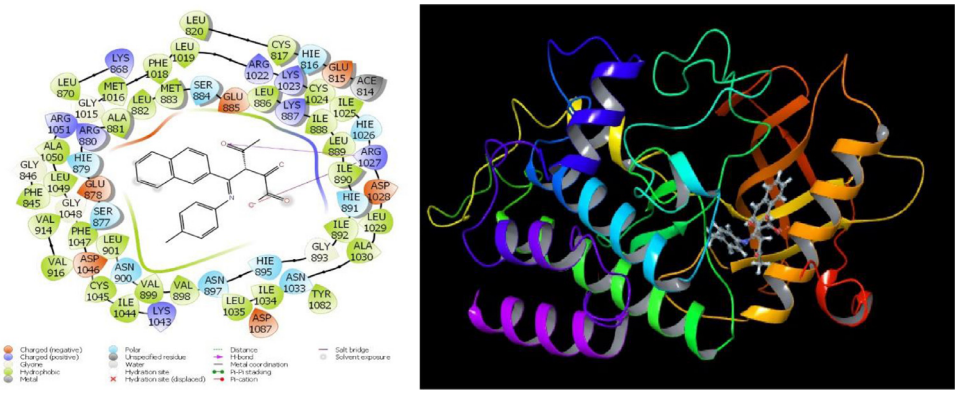

Fig. 5. Interaction presentation of molecule **1** with liver cancer protein.

metabolism is tried to be predicted theoretically. Furthermore, it provides information about how drugs or molecules are absorbed by human tissues and organs and their functioning and excretory processes. Among the parameters to be examined for this analysis, the two most important parameters are RuleOfFive [36,37] and RuleOfThree [38]. These parameters consist of a combination of many parameters. The numerical values of these parameters must be minimum zero and maximum four. ADME properties of molecules are given in Table 4.

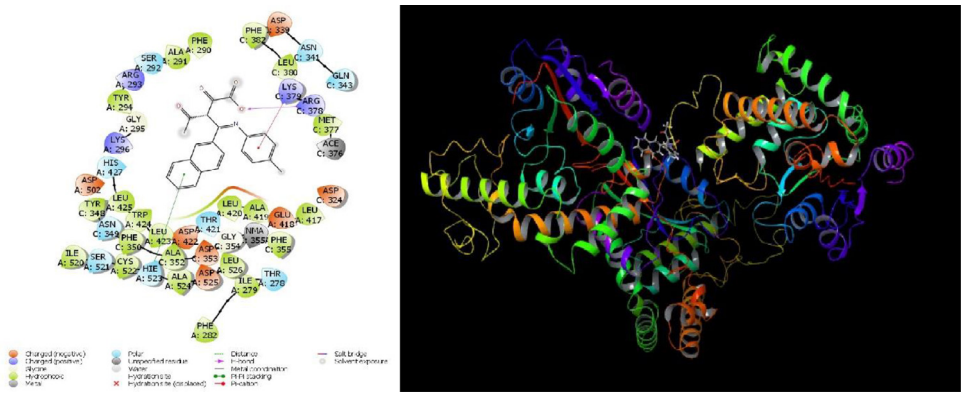

Fig. 6. Interaction presentation of molecule **1** with lung cancer protein.

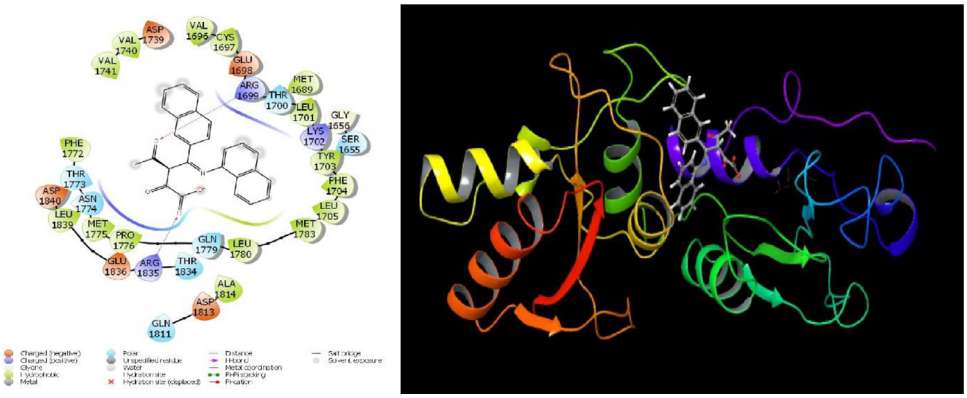

Fig. 7. Interaction presentation of molecule **3** with breast cancer protein.

Table 4
ADME properties of molecules.

	1	2	3	4	5	Reference Ranges
mol_MW	373	404	409	–	464	130–725
dipole (D)	12.6	10.9	6.6	–	8.1	1.0–12.5
SASA	619	633	670	–	698	300–1000
FOSA	119	66	66	–	68	0–750
FISA	167	223	154	–	340	7–330
PISA	334	344	451	–	290	0–450
WPSA	0	0	0	–	0	0–175
volume (A^3)	1140	1167	1239	–	1277	500–2000
donorHB	1	1	1	–	2	0–6
accptHB	6	7	6	–	9	2.0–20.0
glob (Sphere =1)	0.9	0.8	0.8	–	0.8	0.75–0.95
QPpolrz (A^3)	38.2	38.7	43.2	–	41.3	13.0–70.0
QPlogPC16	12.6	13.3	14.2	–	15.0	4.0–18.0
QPlogPoct	19.5	19.9	19.9	–	23.0	8.0–35.0
QPlogPw	10.4	11.7	11.3	–	15.3	4.0–45.0
QPlogPo/w	3.7	3.1	4.5	–	2.0	−2.0–6.5
QPlogS	−4.2	−3.9	−5.1	–	−4.1	−6.5–0.5
CIQPlogS	−5.4	−5.6	−6.3	–	−6.0	−6.5–0.5
QPlogHERG	−3.7	−3.8	−4.6	–	−4.1	*
QPPCaco (nm/*sec*)	66.1	19.2	87.4	–	1.5	**
QPlogBB	−1.4	−2.0	−1.3	–	−3.4	−3.0–1.2
QPPMDCK (nm/*sec*)	33.4	8.8	45.2	–	0.6	**
QPlogKp	−2.7	−3.7	−2.1	–	−5.8	Kp in cm/hr
IP (ev)	9.0	9.1	8.8	–	9.5	7.9–10.5
EA (eV)	1.1	1.6	1.1	–	1.8	−0.9–1.7
#metab	2	3	1	–	2	1–8
QPlogKhsa	0.1	−0.1	0.4	–	−0.2	−1.5–1.5
Human Oral Absorption	3	2	3	–	1	–
Percent Human Oral Absorption	81	68	88	–	29	***
PSA	102	141	98	–	195	7–200
RuleOfFive	0	0	0	–	1	Maximum is 4
RuleOfThree	0	1	0	–	1	Maximum is 3
Jm	0.0	0.0	0.0	–	0.0	–

* concern below −5, ** a<25 is poor and a>500 is great, *** b<25 is poor and b>80 is high.

4. Conclusions

In this study, some organic molecules were synthesized and characterized. All molecules were tested against two different cancer cell lines. A compound (**3**) having naphthyl groups was found to have high activity in breast cancer cell line. After that biological activity values of heterocyclic compounds against cancer proteins were calculated. As a result of the calculations, a different protein was found against each cancer protein when comparing the molecules' biological activities. Compound **4** was found to have the highest biological activity against the breast cancer protein. The activity of compound **3** was found to be the highest in the calculations made based on the B3LYP level in the Gaussian software program. On the other hand, against the remaining two cancer proteins, compound **1** has a higher biological activity value than the others. In the calculations made at the HF and M062X levels, it was found that compound **1** has the highest activity. After examining these heterocyclic compounds' interaction against proteins, ADME/T analysis was performed to evaluate their drug-ability properties. When the parameters obtained from this analysis were examined, there was found to be no harm in using these molecules as medicine. Considering this examination, numerical values of heterocyclic compounds' parameters can be used *in vivo* and *in vitro* studies for future new drug candidate research.

Declaration of Competing Interest

The authors declare that they have no known competing financial interests or personal relationships that could have appeared to influence the work reported in this paper.

Acknowledgments

SA would like to thank Erciyes University Genome and Stem Cell Center (GENKOK) for allowing her to carry out cytotoxic activity studies in its laboratories. BT thanks TUBITAK ULAKBIM for permission to use the High Performance and Grid Computing Center (TR-Grid e-Infrastructure).

Supplementary materials

Supplementary material associated with this article can be found, in the online version, at doi:10.1016/j.molstruc.2021.131127.

References

[1] T. Liu, S. Song, X. Wang, J. Hao, Small-molecule inhibitors of breast cancer-related targets: potential therapeutic agents for breast cancer, Eur J Med Chem. 210 (2021) 112954.
[2] L.A. Chodosh, Breast cancer: current state and future promise, Breast Cancer Res. 13 (2011) 113-113.
[3] C.W.S. Tong, M. Wu, W.C.S. Cho, K.K.W. To, Recent advances in the treatment of breast cancer, Front Oncol 8 (2018) 227.
[4] S.A. Al-Maweri, W.I. Ibraheem, M.S. Al-Ak'hali, A. Shamala, E. Halboub, M.N. Alhajj, Association of periodontitis and tooth loss with liver cancer: a systematic review, Crit. Rev. Oncol. Hematol. 159 (2021) 103221.
[5] F. Bray, J. Ferlay, I. Soerjomataram, R.L. Siegel, L.A. Torre, A. Jemal, Global cancer statistics 2018: GLOBOCAN estimates of incidence and mortality worldwide for 36 cancers in 185 countries, CA Cancer J Clin 68 (2018) 394–424.
[6] M. Thun, M.S. Linet, J.R. Cerhan, C.A. Haiman, D. Schottenfeld, Cancer epidemiology and prevention, New York: Oxford University Press (2018) 635–660.
[7] E. Zigler, M. Eder, C. Belegratis, E.Und Prewedourakis, Synthesen van heterocyclen 103, Mitt: Über Reaktionen mit Oxalychlorit, Monatsh. Chem. 98 (1967) 2249–2251.
[8] H. Üngören, Metil aromatik keton ve etilasetat bileşiklerinden 2,3-furandion bileşiklerinin sentezi, Yüksek Lisans Tezi-Erciyes Üniversitesi-Kayseri. (2000).
[9] S. Akkoç, Derivatives of 1-(2-(Piperidin-1-yl)ethyl)-1H-benzo[*d*]imidazole: synthesis, characterization, determining of electronic properties and cytotoxicity Studies, ChemistrySelect 4 (2019) 4938–4943.
[10] S. Akkoç, Antiproliferative activities of 2-hydroxyethyl substituted benzimidazolium salts and their palladium complexes against human cancerous cell lines, Synth Commun. 49 (2019) 2903–2914.
[11] D. Vautherin, D.M. Brink, Hartree-fock calculations with skyrme's interaction. I. spherical nuclei, Physical Review C 5 (1972) 626–647.
[12] P.J. Stephens, F.J. Devlin, C.F. Chabalowski, M.J. Frisch, Ab initio calculation of vibrational absorption and circular dichroism spectra using density functional force fields, J Phys Chem. 98 (1994) 11623–11627.
[13] K.B. Wiberg, Basis set effects on calculated geometries: 6-311++G** *vs.* aug-c-c-pVDZ, J Comput Chem. 25 (2004) 1342–1346.
[14] A.D. Becke, Density-functional thermochemistry. III. the role of exact exchange, J Chem Phys. 98 (1993) 5648–5652.
[15] E.G. Hohenstein, S.T. Chill, C.D. Sherrill, Assessment of the performance of the M05−2X and M06−2X exchange-correlation functionals for noncovalent interactions in biomolecules, J Chem Theory Comput. 4 (2008) 1996–2000.
[16] M.J. Frisch, G.W. Trucks, H.B. Schlegel, G.E. Scuseria, M.A. Robb, J.R. Cheeseman, G. Scalmani, V. Barone, B. Mennucci, G.A. Petersson, H. Nakatsuji, M. Caricato, X. Li, H.P. Hratchian, A.F. Izmaylov, J. Bloino, G. Zheng, J.L. Sonnenberg, M. Hada, M. Ehara, K. Toyota, R. Fukuda, J. Hasegawa, M. Ishida, T. Nakajima, Y. Honda, O. Kitao, H. Nakai, T. Vreven, J.A. Montgomery, J.E. Peralta, F. Ogliaro, M. Bearpark, J.J. Heyd, E. Brothers, K.N. Kudin, V.N. Staroverov, R. Kobayashi, J. Normand, K. Raghavachari, A. Rendell, J.C. Burant, S.S. Iyengar, J. Tomasi, M. Cossi, N. Rega, J.M. Millam, M. Klene, J.E. Knox, J.B. Cross, V. Bakken, C. Adamo, J. Jaramillo, R. Gomperts, R.E. Stratmann, O. Yazyev, A.J. Austin, R. Cammi, C. Pomelli, J.W. Ochterski, R.L. Martin, K. Morokuma, V.G. Zakrzewski, G.A. Voth, P. Salvador, J.J. Dannenberg, S. Dapprich, A.D. Daniels, O. Farkas, J.B. Foresman, J.V. Ortiz, J. Cioslowski, D.J. Fox, Gaussian 09, revision D.01. Gaussian Inc (2009).
[17] R.D. Dennington, T.A. Keith, C.M. Millam, GaussView 5.0 Wallingford CT, (2009).
[18] PerkinElmer, ChemBioDraw Ultra Version (13.0.0.3015), CambridgeSoft Waltham, MA, U.S.A., (2012).
[19] Chemissan Version 4.43 package, (2016).
[20] L.E. Brus, A simple model for the ionization potential, electron affinity, and aqueous redox potentials of small semiconductor crystallites, J Chem Phys. 79 (1983) 5566–5571.
[21] R.G. Parr, W. Yang, Density Functional Theory of Atoms and Molecules, Oxford University Press, Oxford, 1989.
[22] L. Schrodinger, Small-Molecule Drug Discovery Suite 2019–4, (2019).
[23] R.A. Friesner, R.B. Murphy, M.P. Repasky, L.L. Frye, J.R. Greenwood, T.A. Halgren, P.C. Sanschagrin, D.T. Mainz, Extra precision glide: docking and scoring incorporating a model of hydrophobic enclosure for protein−ligand complexes, J. Med. Chem. 49 (2006) 6177–6196.
[24] L. Schrödinger, Schrödinger release 2019-4: protein preparation wizard; epik, schrödinger, LLC, New York, NY, 2016; impact, schrödinger, LLC, New York, NY, 2016; Prime, Schrödinger, LLC, New York, NY, 2019.
[25] G.M. Sastry, M. Adzhigirey, T. Day, R. Annabhimoju, W. Sherman, Protein and ligand preparation: parameters, protocols, and influence on virtual screening enrichments, J. Comput. Aided Mol. Des. 27 (2013) 221–234.
[26] L. Schrödinger, Schrödinger Release 2019-4: LigPrep, Schrödinger, LLC, New York, NY, 2019 2019.
[27] Q. Du, Y. Qian, X. Yao, W. Xue, Elucidating the tight-binding mechanism of two oral anticoagulants to factor Xa by using induced-fit docking and molecular dynamics simulation, J. Biomol. Struct. Dyn. 38 (2020) 625–633.
[28] L. Schrödinger, Schrödinger Release 2020-1: QikProp, Schrödinger, LLC, New York, NY, 2020, (2020).
[29] B. Tüzün, Investigation of pyrazoly derivatives schiff base ligands and their metal complexes used as anti-cancer drug, Spectrochim. Acta. A: Mol. Biomol. Spectrosc. 227 (2020) 117663.
[30] H. Genc Bilgicli, P. Taslimi, B. Akyuz, B. Tuzun, İ. Gulcin, Synthesis, characterization, biological evaluation, and molecular docking studies of some piperonyl-based 4-thiazolidinone derivatives, Arch. Pharm. (Weinheim) 353 (2020) 1900304.
[31] K. Sayin, D. Karakaş, Determination of structural, spectral, electronic and biological properties of tosufloxacin boron complexes and investigation of substituent effect, J Mol Struct 1146 (2017) 191–197.
[32] K. Sayin, D. Karakaş, Investigation of structural, electronic properties and docking calculations of some boron complexes with norfloxacin: a computational research, Spectrochim Acta A: Mol. Biomol. Spectrosc. 202 (2018) 276–283.
[33] K. Sayin, A. Üngördü, Investigation of anticancer properties of caffeinated complexes via computational chemistry methods, Spectrochim Acta A. Mol. Biomol. Spectrosc. 193 (2018) 147–155.
[34] P. Taslimi, Y. Erden, S. Mamedov, L. Zeynalova, N. Ladokhina, R. Tas, B. Tuzun, A. Sujayev, N. Sadeghian, S.H. Alwasel, I. Gulcin, The biological activities, molecular docking studies, and anticancer effects of 1-arylsuphonylpyrazole derivatives, J. Biomol. Struct. Dyn., (2020) 1–11.
[35] H.U. Celebioglu, Y. Erden, F. Hamurcu, P. Taslimi, O.S. Şentürk, Ü.Ö. Özmen, B. Tuzun, İ. Gulçin, Cytotoxic effects, carbonic anhydrase isoenzymes, α-glycosidase and acetylcholinesterase inhibitory properties, and molecular docking studies of heteroatom-containing sulfonyl hydrazone derivatives, J. Biomol. Struct. Dyn.. (2020) 1–12.
[36] C.A. Lipinski, Lead- and drug-like compounds: the rule-of-five revolution, Drug Discov. Today Technol. 1 (2004) 337–341.
[37] C.A. Lipinski, F. Lombardo, B.W. Dominy, P.J. Feeney, Experimental and computational approaches to estimate solubility and permeability in drug discovery and development settings, Adv. Drug Deliv. Rev.. 23 (1997) 3–25.
[38] W.L. Jorgensen, E.M. Duffy, Prediction of drug solubility from structure, Adv Drug Deliv Rev. 54 (2002) 355–366.